Published in final edited form as:
Exp Gerontol. 2012 May ; 47(5): 361–371. doi:10.1016/j.exger.2012.02.008.

Calorie restriction in mice overexpressing UCP3: evidence that prior mitochondrial uncoupling alters response

Carmen Estey[*], **Erin L. Seifert**[*,1], **Céline Aguer**, **Cynthia Moffat**[1], and **Mary-Ellen Harper**
Dept. Biochem Microbiol Immunol, University of Ottawa, Ottawa, ON K1H 8M5

SUMMARY

Calorie restriction (CR) without malnutrition is the only intervention to consistently increase lifespan in all species tested, and lower age-related pathologies in mammals including humans. It has been suggested that uncoupling of mitochondrial oxidative phosphorylation, using chemical uncouplers, mimics CR, and that overlapping mechanisms underlie the phenotypic changes induced by uncoupling and CR. We aimed to critically assess this using a unique mouse model of skeletal muscle-targeted UCP3-induced uncoupling (UCP3Tg), and focused our studies mainly on skeletal muscle mitochondria. Compared to *ad libitum* fed Wt mice, skeletal muscle mitochondria from *ad libitum* fed UCP3Tg mice showed higher basal uncoupling and lower H_2O_2 emission, with unchanged maximal oxidative phosphorylation, and mitochondrial content. UCP3Tg CR mice showed some tendency for differential adaptation to CR, with lowered H^+ leak conductance and evidence for higher H_2O_2 emission from skeletal muscle mitochondria following 2 weeks CR, and failure to lower H_2O_2 emission after 1 month CR. Differential adaptation was also apparent at the whole body level: while UCP3Tg CR mice lost as much weight as Wt CR mice, the proportion of muscle lost was higher in UCP3Tg mice. However, a striking outcome of our studies was the absence of change with CR in many of the parameters of mitochondrial function and content that we measured in mice of either genotype. Overall, our study raises the question of whether CR can consistently modify skeletal muscle mitochondria; alterations with CR may only be apparent under certain conditions such as during the 2 wk CR intervention in the UCP3Tg mice.

Keywords

uncoupling proteins; oxidative phosphorylation; oxidative stress; mitochondrial biogenesis; indirect calorimetry

Correspondence to: Dr. M-E Harper, Professor, Department of Biochemistry, Microbiology and Immunology, Faculty of Medicine, University of Ottawa, 451 Smyth Rd., Ottawa, ON, Canada K1H 8M5. Tel: +1-613-562-5800 ext 8235, Fax: +1-613-562-5452.
[*]These authors contributed equally to this work
[1]Current address: Thomas Jefferson University, Dept Pathology, Anatomy and Cell Biology, Philadelphia, PA, USA 19107

Author Contributions
Study design: CE, ELS, MEH; data collection: CE, ELS, CA, CM; data analysis: CE, ELS, MEH; wrote manuscript: CE, ELS, MEH.

1. INTRODUCTION

Calorie restriction (CR) without malnutrition is the only intervention that markedly and consistently increases lifespan in all species tested and lowers age-related pathologies or biomarkers of aging in mammals (for review: (Smith et al., 2010)), including humans (Heilbronn et al., 2006). Thus, it is of interest to understand the mechanisms by which CR modifies organismal physiology, particularly in light of current efforts to develop CR mimetic compounds (Chen and Guarente, 2007; Ingram et al., 2006; Smith et al., 2010). The possibility that uncoupling of mitochondrial oxidative phosphorylation, through the use of chemical uncouplers, can mimic CR has been considered, as has the possibility that phenotypic changes induced by uncoupling and CR depend on similar mechanisms (Caldeira da Silva et al., 2008; Mookerjee et al., 2010). More generally, CR has been associated with remodelling of the mitochondrial mass (Barazzoni et al., 2005; Bevilacqua et al., 2004, 2005; Civitarese et al., 2007; Marzetti et al., 2008; Nisoli et al., 2005) (Asami et al., 2008), leading to the general idea that alterations in mitochondrial content and function underlie at least some of the effects of CR (Guarente, 2008). Whether this is indeed the case in all tissues is as yet unclear, and has been very recently challenged (Hancock et al., 2011).

Mitochondrial uncoupling induces several phenotypic changes that are hallmarks of CR. In this regard, CR has been associated with decreases in reactive oxygen species (ROS) production and indicators of oxidative stress (Asami et al., 2008; Bevilacqua et al., 2005; Heilbronn et al., 2006; Lass et al., 1998). Mitochondrial ROS generation can be mitigated by (as yet poorly characterized) mechanisms that decrease the protonmotive force across the mitochondrial inner membrane (Caldeira da Silva et al., 2008; Korshunov et al., 1997; Seifert et al., 2010). Specifically, low-dose uncoupler treatment of mice decreased the levels of H_2O_2 in brain, liver and heart, and of DNA and protein oxidation in these tissues (Caldeira da Silva et al., 2008). Another hallmark of CR is enhanced insulin sensitivity, and decreased plasma glucose, insulin and triglycerides (*e.g.*, (Heilbronn et al., 2006)), and such changes also occur in mice treated with low-doses of uncoupler (Caldeira da Silva et al., 2008) or with muscle-specific UCP1 overexpression (Gates et al., 2007; Katterle et al., 2008; Li et al., 2000; Neschen et al., 2008). Regarding lifespan extension, the effects of induced uncoupling are mixed, with studies showing an increase in maximal lifespan (Caldeira da Silva et al., 2008) or no change (Gates et al., 2007) in mice, and an increase in mean (but not maximal) lifespan of uncoupler-treated flies (Padalko, 2005) or flies with neuronal expression of human UCP2 (Fridell et al., 2005). Also consistent with a role for uncoupling in lifespan extension is the finding that outbred mice with the highest metabolic rate had higher H^+ conductance in skeletal muscle mitochondria and survived the longest (Speakman et al., 2004).

While the above studies suggest that uncoupling mimics CR, whether endogenous uncoupling, by a protein that is native to skeletal muscle, would mimic CR is not known and was the original aim of this study. We specifically tested whether muscle-specific overexpression of UCP3, which increases basal H^+ leak in ad *libitum* fed mice, functioned as a CR mimetic. We focused on the impact of CR on whole body energetics and skeletal muscle mitochondrial mass and function. Based on studies of skeletal muscle mitochondrial function in CR rats and observations of CR effects on mitochondria from other tissues, we

expected that CR would increase mitochondrial content and decrease ROS in Wt mitochondria. We used two durations of short-term CR, and investigated many parameters of skeletal muscle mitochondrial function as well as protein expression and mitochondrial content. Surprisingly, our most important finding is that CR does not greatly impact skeletal muscle mitochondria in mice. Observations also point to an altered response to acute CR in mice overexpressing UCP3. In particular, results suggest an attempt of the muscle to offset the higher leak-dependent respiration, at least during the early phase of CR.

2. EXPERIMENTAL PROCEDURES

2.1. Animals and diets

Male C57BL/6J wild–type (Wt) and UCP3 transgenic (UCP3Tg) mice were used in this study. The human α–skeletal muscle actin promoter was used to drive skeletal muscle-specific expression of the human UCP3 transgene (Clapham et al., 2000). UCP3Tg mice were backcrossed 10 generations into the C57BL/6J background. At 8 wk of age, individually housed Wt and UCP3Tg mice were switched to the AIN-93M control rodent diet (D01092701: Research Diets, New Brunswick, NJ) which they were fed *ad libitum*. From 8 – 12 wk of age, body weight (BW) and food intake were determined twice/wk. At 12 wks of age, mice were randomized into control (*ad libitum*: AL) or 40% calorie restricted (CR) treatment groups. Mice in the AL group remained on the control diet and were subsequently given an average of their *per diem* food intake each day, calculated over the preceding 4 wks. Mice in the CR group were fed a custom CR diet (D01092702, Research Diets, New Brunswick, NJ, USA) enriched in vitamins and minerals and macronutrients with the exception of corn starch and maltodextrin such that the feeding of 60% of their *ad libitum* food intake resulted in a 40% reduction in dietary energy and unaltered intakes of other nutrients. The AL and CR treatments lasted 2 wk or 1 mo. Throughout the study, all mice were given free access to water, and kept at 24°C in a 12:12-h light-dark cycle (lights on: 06:00–18:00). All BW determinations and daily feeding were conducted between 16:00–16:30. Mice were 14 or 16 wk of age at sacrifice, corresponding to the 2 wk and 1 mo CR interventions, respectively. All mice were cared for according to the principles and guidelines of the Canadian Council on Animal Care and the Institute of Laboratory Animal Resources (National Research Council, Canada). Approval of this study came from the Animal Care Committee of the University of Ottawa.

2.2. Indirect calorimetry

Indirect calorimetry was performed using a customized 4-chamber Oxymax open-circuit indirect calorimeter (Columbus Instruments, Columbus, OH). Two days prior to sacrifice, mice were placed individually in 2.5-L Plexiglass chambers supplied with air at 0.5 L/min, and maintained at 24°C with lights on from 06:00 to 18:00. In each chamber, concentrations of O_2 and CO_2 in dry air were measured for 60 sec/9 min, with a sample line-purge time of 2 min. All mice were acclimated to the chamber for 2 hr prior to data collection starting at 16:00. Whole body O_2 consumption (VO_2), and CO_2 production (VCO_2) data were collected over 24-h periods. The respiratory exchange ratio (RER) was calculated as $V\,CO_2/VO_2$.

2.3. Organ weights

From each mouse the heart, liver, kidneys, gonadal white adipose tissue (gWAT) and interscapular brown adipose tissue (iBAT) were carefully dissected, blotted dry, and weighed.

2.4. Isolation of skeletal muscle mitochondria

Isolation of skeletal muscle mitochondria was performed using a modified method of Chappell and Perry (Chappell and Perry, 1954), as described (Seifert et al., 2010). Mitochondrial preparations were obtained from skeletal muscle from the forelimbs, hind limbs and the pectoral region; all muscle groups were harvested. The protein concentration of each sample was determined using a modified Lowry protein assay, with BSA as the standard.

2.5. Mitochondrial content

Mitochondrial yield was determined by normalizing the mitochondrial protein concentration to the wet muscle weight obtained. Mitochondrial content was also estimated by histochemical activity staining for cytochrome c oxidase (COX), obtained from a section of the *vastus lateralis* (Dubowitz, 2007). Slides were individually visualized by light microscopy using a 20X objective. All images were captured using the same lighting and exposure settings, and analyzed by obtaining the integrated pixel density per muscle fiber along with the total area of each muscle fiber, using ImageJ (NIH). The total integrated density (background-corrected) for the whole region of muscle was normalized to total fiber area.

2.6. Mitochondrial oxygen consumption

Oxygen consumption of isolated mitochondria was measured using a Clark-type oxygen electrode (Hansatehc, Norfolk, UK). Mitochondria (0.25 mg/mL) were stirred at 37°C in incubation media (IM: 120mM KCl, 5mM HEPES, 5mM $MgCl_2$, 1mM EGTA, 5mM KH_2PO_4 and 0.3% BSA (w/v); pH 7.4 at 25°C). Pyruvate (5mM) and malate (2.5mM), or palmitoyl-L-carnitine (PC; 18μM) and malate (0.5mM) were used as substrates, and ADP (200μM) was added to stimulate state 3 respiration. Oligomycin (8μg/mg mitochondria) inhibited the ATP synthase, and carbonyl cyanide–p-trifluoromethoxyphenylhydrazone (FCCP; 0.3μM) was added to maximally uncouple mitochondria.

2.7. Mitochondrial proton leak

Non-phosphorylating mitochondrial O_2 consumption at a given protonmotive force (PMF) was determined by measuring PMF and O_2 consumption in parallel. Oxygen consumption was measured as described above. PMF was detected fluorimetrically using 5μM safranin O (excitation 485nm, emission 580nm) (Seifert et al., 2010), at 37°C in IM. Proton leak of isolated mitochondria (0.3mg/mL) was determined in the presence of rotenone (5 μM), nigericin (0.4μg/mL), oligomycin (8μg/mg mitochondria), with succinate (10mM) as substrate followed by 5 successive 1mM additions of malonate, then FCCP (0.3μM). State 4 respiration (maximal non-phosphorylating respiration) was measured prior to malonate addition, and is depicted as the rightmost point on the leak curves.

2.8. Mitochondrial ROS production

The p-hydroxyphenyl acetic acid (PHPA)/horseradish peroxidase (HRP) assay (Seifert et al., 2010) was used to assess ROS formation in isolated skeletal muscle mitochondria. H_2O_2 was detected fluorimetrically (excitation: 320nm; emission: 400nm) using a temperature-controlled microplate fluorescence reader (FLx 800, Biotek, Winooski, VT), at 37°C. PHPA (167μg/mL), HRP (9 units/mL), superoxide dismutase (20units/mL), and isolated mitochondria (0.3mg/mL) were suspended in warmed IM. Addition of superoxide dismutase to all reactions resulted in conversion of the superoxide formed on the intermembrane space side of the inner membrane into H_2O_2. Depending on the experimental conditions, antimycin A (5μM), rotenone (5μM), and oligomycin (8μg/mg mitochondria) were also added. Reactions were initiated by addition of substrate: PC (18μM), pyruvate/malate (5mM/2.5mM) or succinate (10mM). H_2O_2 production was determined as nmol H_2O_2/min/mg mitochondria by the use of a standard curve generated in the presence of mitochondria.

2.9. Western blotting

The level of 4-HNE protein adducts within a cell provides a measure of oxidative damage; in particular, we used a 4-HNE antibody that recognizes an acetyl-lysine-4-HNE conjugate (Tsai et al., 1998). Samples were loaded at 30μg of protein per lane for 4-HNE and UCP3, or 15μg of protein per lane for MnSOD and ANT. The following primary antibodies were used: MnSOD (1:2,000; rabbit polyclonal IgG: sc-30080, Santa Cruz Biotechnology), 4–HNE (1:2,500; rabbit polyclonal IgG: 393206, Calbiochem-EMD4 Biosciences, Gibbstown, NJ), ANT (1:4,000; goat polyclonal IgG: sc-9299, Santa Cruz Biotechnology Inc., Santa Cruz, CA) and UCP3 (1:1,000; rabbit polyclonal IgG, Abcam, Cambridge, MA). Secondary antibodies were goat anti-rabbit IgG-HRP (1:1000; sc-2030, Santa Cruz Biotechnology) and donkey anti-goat IgG-HRP (1:1000; sc-2033, Santa Cruz Biotechnology). Protein bands were detected by enhanced chemiluminescence (ECL RPN 2109: GE Healthcare, Baie d'Urfé, Qc, Canada) and subsequent exposure onto film (Polaroid Polapan–667) or imaging (Typhoon Trio, GE Healthcare). Band intensity was quantified as the integrated pixel intensity using ImageJ (NIH). Coomassie stained gels were used as loading controls; gels were scanned, and pixel intensity of a series of bands was determined as above.

2.10. Statistical analysis

Comparisons between Wt AL and UCP3Tg AL mice were analyzed by two–tailed, unpaired t–tests (Microsoft Office Excel 2003), or two-way analysis of variance (independent samples) were performed with Bonferroni *posthoc* contrasts (Prism, Graph Pad, La Jolla, CA), as appropriate. Confidence intervals for the CR response were calculated using the standard deviation (SD) for the difference between two means: $\mathrm{sqrt}[((s1^2)/n1)+((s2^2/n2)]$; where s1 = SD for sample 1, s2 = SD for sample 2, n1 = size of sample 1, n2 = size of sample 2. Statistical significance was defined as $P<0.05$. All data are presented as mean ± standard error of the mean (SEM).

3. RESULTS

3.1. Basal H^+ leak and ROS production in Wt and UCP3Tg skeletal muscle mitochondria

UCP3 protein was ~250% higher in skeletal muscle mitochondria from UCP3Tg mice ($P<0.0005$; Fig. 1A). As previously reported (Bezaire et al., 2005; Costford et al., 2008; Costford et al., 2006), UCP3Tg mice weighed less than Wt mice, despite similar per mouse food intake or increased food intake if normalized to BW (Table 1); the lower body weight (BW) of UCP3Tg mice was due in part to reduced muscle mass. Moreover, the feed efficiency [(weight gain*day^{-1}/food intake*day^{-1})*100] was lower in UCP3Tg mice (4.4±0.2% *vs.* 3.3±0.4% in Wt *vs.* Tg, P=0.05, n=14 and 18, respectively). Whole-body $\dot{V}O_2$ was similar higher in UCP3Tg mice (Suppl. Fig. 1). Some metabolic characteristics of *ad libitum* (AL)-fed Tg mice from our lab have been described (Bezaire et al., 2005; Costford et al., 2008; Costford et al., 2006). Here we report further characterization relevant to the present study, namely H^+ leak kinetics and ROS production in skeletal muscle mitochondria.

To assess H^+ leak kinetics in skeletal muscle mitochondria, O_2 consumption and PMF (protonmotive force) were determined in parallel (Fig. 1B). No difference in state 4 respiration (rightmost point) or in corresponding PMF was observed between genotypes. Titration with malonate, a competitive inhibitor of succinate dehydrogenase, displaced the UCP3Tg curve leftward relative to the Wt curve such that at a given PMF, O_2 consumption was higher in UCP3Tg. Quantification at a common PMF yielded O_2 consumption that was ~40% higher in UCP3Tg mitochondria ($P<0.001$, Fig. 1B). Similar observations were made using a $TPMP^+$-selective electrode to obtain quantitative determinations of H^+ leak kinetics (Suppl. Fig. 2).

Based on increased leakiness of skeletal muscle mitochondria from UCP3Tg mice, it was of interest to determine mitochondrial ROS production, measured as H_2O_2 emission. Measurements were undertaken in state 4 using palmitoy-L-carnitine (PC) as the substrate; a PMF is generated in this condition. To gain further insight into mechanism(s) underlying differential ROS production capacity in UCP3Tg and Wt mitochondria, H_2O_2 emission was also evaluated in the presence of complex I or III inhibitors (conditions in which little PMF is generated), and with non-lipid substrate (pyruvate/malate (P/M), succinate). UCP3Tg mitochondria emitted less H_2O_2 than Wt mitochondria, independently of PMF, the inhibitor used, or whether mitochondria oxidized PC or P/M (Fig. 1C). The only condition for which there was no significant difference was when succinate was oxidized in the presence of rotenone and antimycin (yielding ROS primarily at complex III). Overall, the capacity for ROS production was clearly lower in UCP3Tg compared to Wt mitochondria, independent of substrate catabolic pathways. That abundance of complexes I and III, as well as MnSOD expression (see Fig. 3c and 4b) are similar between Wt and UCP3Tg mice indicate that the lower ROS in UCP3Tg is also independent of the ROS generating capacity of complexes I and III, as well as the capacity to convert superoxide to H_2O_2.

3.2. Whole body responses to 2 wk or 1 mo CR in UCP3Tg and Wt mice

Based on previous studies in rats from our laboratory (Bevilacqua et al., 2005), we expected 2 wk CR to be associated with lowered ROS in skeletal muscle mitochondria in mice; thus,

the present study initially focused on a 2 wk CR intervention. Interestingly, we found here (see below), as well as in another study (Bevilacqua et al., 2010) that ROS production was unchanged following 2 wk CR in Wt mice. The discrepant results in rats and mice have been discussed (Bevilacqua et al., 2010). Because the 2 wk intervention was nonetheless informative, we continued to investigate this condition. In addition, we also investigated a longer CR intervention (1 mo), which resulted in lowered ROS in skeletal muscle mitochondria from Wt mice.

Body and organ weights and body composition—Total BW of Wt and UCP3Tg mice was similarly decreased by CR lasting 2 wk (~ 25% drop) or 1 mo (~ 36% drop), due to decreases in the weight of kidneys, liver, gWAT, iBAT and skeletal muscle (Tables 1 and 2, upper panels). Two wk and 1 mo CR effects on body composition were assessed by determining organ weights as a percentage of BW (Tables 1 and 2, lower panels). After 2 wk CR, there was a more pronounced decrease in muscle (2-way ANOVA, interaction: $P = 0.0003$; Bonferroni post hoc: $P<0.001$), iBAT (2-way ANOVA, interaction: $P = 0.0019$; Bonferroni post hoc: $P<0.001$), and a tendency for a greater decrease in gWAT (2-way ANOVA, interaction: $P = 0.07$; Bonferroni post hoc: $P<0.05$), in UCP3Tg mice. In contrast to 2 wk CR, while 1 mo CR altered the body composition in both genotypes (2-way ANOVA, significant main effect of diet, see Table 2), the changes were similar in Wt and UCP3Tg CR mice.

Whole animal energetics—On a per mouse basis, both 2 wk and 1 mo CR significantly decreased VO_2 in both genotypes, during both light and dark phases (2-way ANOVA, main effect of diet: $P<0.001$ for light and dark phases, for both 2 wk and 1 mo CR, Figure 2A, B, top panels); the interaction term was not significant; thus the CR effect was similar in both genotypes. To account for the differential effect of 2 wk CR on body composition in UCP3Tg and Wt mice, VO_2 data was expressed relative to fat free mass (FFM; measured as the combined weight of skeletal muscle, liver, heart, and kidneys) in each mouse (Fig 2A, B, bottom panels). Normalization to FFM resulted in lower VO_2 in 2 wk CR mice (2-way ANOVA, main effect of diet: $P = 0.008$ for light phase, $P < 0.001$ for dark phase). This normalization also resulted in a small but significant main effect of genotype, such that VO_2 in the UCP3Tg mice was higher ($P = 0.003$ for light phase, $P = 0.015$ for dark phase). However, the interaction term was not significant; thus the effect of CR on VO_2 was similar in Wt and UCP3Tg mice. Similar patterns were apparent when the indirect calorimetry data were normalized by skeletal muscle mass (Suppl. Table 1). In 1 mo CR mice, normalization to FFM only resulted in a significant main effect of diet in the dark phase only ($P < 0.04$). Normalization to BW was also performed (Suppl. Fig. 3), yielding no differences between genotypes in the light phase (2 wk or 1 mo CR), but a similar decrease in dark phase values from 2 wk CR UCP3Tg and Wt mice ($P<0.05$). The RER in CR (2 wk or 1 mo; Fig. 2C, D) mice rapidly decreased from ~1.0 to ~0.7 during the second half of the dark phase, whereas RER in AL control mice remained at ~1.0 for most of the dark phase. The extent and kinetics of the changes in RER were similar in CR UCP3Tg and Wt mice.

In summary, there were some quantitative differences between the genotypes in how they responded at a whole-body level to CR. Ultimately, however, the Wt and UCP3Tg mice

generally responded similarly to CR in terms of whole body energetics and substrate utilization.

3.3. Changes in skeletal muscle mitochondria from UCP3Tg and Wt mice challenged with 2 wk or 1 mo CR

Mitochondrial content—Skeletal muscle mitochondrial content was determined as *in situ* complex IV activity in frozen sections of *vastus lateralis* muscle and as yield of mitochondria recovered from all limb muscles. In both genotypes *in situ* complex IV activity was unchanged with 2 wk CR (Fig. 3A), but was decreased with 1 mo CR independently of genotype (main effect of diet: $P = 0.005$) (Fig. 3A). There was no change in yield (% of muscle wet weight) with 2 wk or 1 mo CR (Fig. 3B). Mitochondrial content was further assessed by measuring levels of TCA cycle and ETC proteins in muscle homogenates from 1 mo CR mice; in both genotypes, levels of five different proteins were similar between AL and CR (Fig. 3C). It should be noted that Wt and UCP3Tg samples were run on separate gels; therefore comparisons between genotypes is not possible. However, side by side comparisons of mitochondria from AL Wt and UCP3Tg revealed similar levels of complex III (Aguer *et al*., unpublished).

ROS production—Because CR decreases ROS production in skeletal muscle mitochondria from rats (Bevilacqua et al., 2005), similar observations were expected in Wt mice. On the other hand, since mitochondria from UCP3Tg mice already had lowered ROS production compared to Wt (Fig. 1C), it was hypothesized that CR would have little effect on ROS production in mitochondria from UCP3Tg mice. Surprisingly, and in contrast to effects in rats, ROS production in Wt mitochondria was unaffected by 2 wk CR, under any conditions tested (Fig. 4A). Interestingly, ROS production tended to be higher after 2 wk CR in UCP3Tg mitochondria. This reached significance only with fatty acid substrate +antimycin (2-way ANOVA, significant main effects of diet [$P = 0.054$] and genotype [$P = 0.018$]; $P<0.05$ for the 99% confidence interval constructed for the CR response in Wt *vs*. UCP3Tg). For the oligomycin condition, which most closely approximates what could occur *in vivo*, both genotype and diet main effects of the 2-way ANOVA were significant, and a change (increase) with CR is more apparent in Tg than in Wt mitochondria; however, neither the interaction term of the ANOVA nor analysis of confidence intervals for the CR response yielded significance. Two wk CR had little effect on 4-HNE protein adduct levels in mitochondrial proteins from either genotype (data not shown). Differently from the 2 wk CR treatment, 1 mo CR lowered ROS production in Wt mitochondria oxidizing PC +antimycin (2-way ANOVA, significant main effects for diet: $P = 0.015$; $P<0.05$ for the 97.5% confidence interval for the CR response in Wt vs. UCP3Tg; (Fig. 5A)). There were however no CR-induced changes in ROS production in mitochondria from UCP3Tg mice. As with 2 wk CR, levels of 4–HNE protein adduct formation on mitochondrial proteins were unchanged with 1 mo CR in both Wt and UCP3Tg muscle mitochondria (data not shown).

Antioxidant protein expression—Given the trend for higher ROS production in mitochondria from UCP3Tg mice after 2 wk CR and in light of the decreased ROS production in mitochondria from 1 mo CR Wt mice, we investigated levels of antioxidant proteins in skeletal muscle mitochondria (Fig. 4B and 5B). In the 2 wk CR intervention,

both Wt and UCP3Tg mitochondrial levels of UCP3 protein were unaltered, but increased in Wt mitochondria following 1 mo CR (2-way ANOVA, significant diet X genotype: $P = 0.027$; Bonferroni post hoc: $P < 0.05$). Two wk CR had no effect on ANT protein levels in Wt mitochondria, but lowered ANT protein in UCP3Tg mitochondria (2-way ANOVA, main effect of diet; $P<0.05$ for 99% confidence intervals for the CR response in Wt vs. UCP3Tg). ANT protein was unaltered by 1 mo CR in mitochondria from either genotype. ANT was of interest in the context of antioxidant defence due to its role in setting the rate of non-phosphorylating respiration, which mitigates ROS production by lowering the mitochondrial membrane potential (*i.e.*, by shifting the redox state of the electron transport chain) (Brand et al., 2005). Levels of MnSOD protein were unaffected by 2 wk or 1 mo CR in either genotype.

Mitochondrial bioenergetics—Using P/M as the substrate, 2 wk CR had little effect on state 3 or 4 respiration rates in either genotype (Fig. 4C). After 1 mo CR, the state 3 rate was similarly decreased in mitochondria from both genotypes (2-way ANOVA, significant main effects of diet [$P = 0.013$] and genotype [$P = 0.013$])(Fig. 5C, top panels). In light of the decreased ROS in mitochondria from 1 mo CR Wt mice (Fig. 5A), respiration rates were also tested using PC as the substrate (Fig. 5C, bottom panels); significant changes were not found with CR.

H^+ leak kinetics—Because H^+ leak may mitigate ROS production and augment whole-body energy consumption, we determined H^+ leak kinetics in muscle mitochondria from AL and UCP3Tg mice after 2 wk or 1 mo CR. With either CR intervention, in Wt mice the leak curves from AL and CR mitochondria overlapped (Fig. 4D, 5D). However in UCP3Tg mice, with 2 wk CR, the leak curve was displaced to the right relative to the AL curve (Fig. 4D); analysis at a common PMF yielded lower O_2 consumption in UCP3Tg CR mitochondria ($P<0.05$). In contrast, 1 mo CR was without effect on H^+ leak kinetics in UCP3Tg mitochondria (Fig. 5D).

4. DISCUSSION

In this study we addressed the question of whether CR and uncoupling share common mechanisms in muscle, a question that is of interest given current efforts to develop CR-mimetic compounds (Chen and Guarente, 2007; Ingram et al., 2006; Smith et al., 2010) and evidence that induced uncoupling mimics CR (Caldeira da Silva et al., 2008; Mookerjee et al., 2010). Overall, when CR resulted in changes in the parameters of interest, similar changes occurred in Wt and UCP3Tg mice. In a few cases, differential responses were observed (summarized in Suppl. Table 2), namely in some measures of ROS emission (2 wk and 1 mo CR); in leak-dependent respiration (2 wk CR); and in body composition changes (2 wk CR). The UCP3Tg mice displayed an early response to CR that effectively pushed their phenotype closer to that of AL-fed Wt mice. Interestingly, following a further 2 wk of CR, fewer differences in CR responses were apparent between UCP3Tg and Wt mice. Thus, it is tempting to speculate that aspects of the UCP3Tg phenotype delayed (part of) the adaption to CR. However, a striking outcome of our study is the minimal changes in skeletal muscle mitochondrial function and content with either the 2 wk or the 1 mo CR. Overall, and to the extent that we can draw conclusions from the few changes we observed in skeletal

muscle mitochondria, we conclude that adaptive responses to uncoupling and CR do not completely share the same mechanistic basis. Different responses would originate from alternative mechanisms of even additive responses. Our overall conclusion generally concurs to that of Asami *et al*. who determined proton leak in skeletal muscle mitochondria as a function of age, and concluded that changes in proton leak in muscle are not responsible for CR-induced changes in lifespan (Asami et al., 2008). It should be noted that their mouse model differed from our model; their model was characterized by overexpression of both UCP2 and UCP3, with overexpression of UCP2 presumably occurring in various tissues in which UCP2 is normally expressed. In addition, they calorie restricted their control mice but not the UCP2/3 overexpressing mice. Thus, their model and experimental design were distinct from ours. Yet, the general conclusions were similar.

4.1. UCP3Tg mice

Skeletal muscle of muscle-specific UCP3Tg mice is characterized by elevated basal H^+ leak and lower ROS production in mitochondria (present study). Previous studies also revealed lower triglyceride stores (Bezaire et al., 2005; Costford et al., 2006). At the whole-body level, BW and efficiency of energy conversion are decreased (present study; (Choi et al., 2007; Clapham et al., 2000; Costford et al., 2006; Tiraby et al., 2007)). Thus, the phenotypic changes in muscle are significant enough to impact whole-body energy balance. However, it is noteworthy that significant aspects of mitochondrial function in UCP3Tg AL mice are similar to Wt AL mice, such as state 3 respiration using different substrates (present study), levels of anti-oxidant proteins and the extent of oxidative modification of mitochondrial proteins (present study). The latter argue against major perturbations in mitochondrial, as well as muscle function due to non-specific effects of overexpression of a mitochondrial inner membrane protein. That increased locomotor activity could explain the lower efficiency of energy conversion seems unlikely; although, we did not directly measure activity, similar variability in the indirect calorimetry data was seen in both UCP3Tg and Wt mice during not only the light phase but also the dark phase when mice are more active (data not shown), suggesting that activity levels were similar in the two genotypes. Other studies have directly measured activity and found no differences between Wt and UCP3Tg mice (Choi et al., 2007; Clapham et al., 2000). Unlike the mice studied by Clapham (Clapham et al., 2000), with roughly 20-fold normal levels of UCP3 expression in muscle, the mice used here and elsewhere (Bezaire et al., 2005; Costford et al., 2006) had much lower levels of overexpression and were not hyperphagic. Whether these energy balance and muscle phenotypes reflect changes in basal uncoupling or UCP3 activation or both is unclear. Our interest was in the higher basal uncoupling and lower ROS production of skeletal muscle mitochondria from UCP3Tg AL mice. However, it is theoretically possible that differences in the response to CR of UCP3Tg mice were driven not by the mitochondrial effects, *per se*, of UCP3 overexpression but rather by other differences in these mice; yet it is worth noting that the differences in whole-body energy balance, though significant, were quite small.

4.2. CR effects on skeletal muscle mitochondria

We were unable to detect an increase with CR in mitochondrial content, as assessed by three independent methods (Fig. 3). Moreover, we observed lower state 3 with P/M in 1 mo Wt CR and UCP3Tg CR mouse mitochondria, and failed to find an increase in state 3 with PC

(Fig. 5C), despite a greater reliance on fatty acids in CR mice (Fig. 2C). In agreement, enzyme activities were lower in skeletal muscle homogenates from mice on CR for ≥ 5 mo (Baker et al., 2006). Also, mitochondrial yield was lower in hearts from rats on CR for 4.5 mo (Lambert et al., 2004), and in triceps from rats that underwent 3 mo CR, key mitochondrial proteins were unchanged at either mRNA or protein levels (Hancock et al., 2011). In rat *gastrocnemius*, while gene expression analysis revealed an upregulation of several oxidative phosphorylation genes with CR (9 mo), this did not translate into a global increase in mitochondrial function (Sreekumar et al., 2002). As well, gene expression profiling in mouse *gastrocnemius* failed to reveal differences in oxidative phosphorylation or other mitochondrial genes with long term CR (Lee et al., 1999). Interestingly, the latter study concluded that the predominant effect of CR in skeletal muscle was a metabolic shift toward increased biosynthesis and macromolecular turnover. The latter is consistent with the preservation of muscle mass in Wt CR mice of our study, as well as in other studies in mice, rats, monkeys and humans (Colman et al., 2009; Faulks et al., 2006; Heilbronn et al., 2006; McKiernan et al.; McKiernan et al.), and in general supports a protective effect of CR against sarcopenia (Evans, 1995; Marzetti et al., 2008). In rhesus monkeys, despite an effect of long-term CR (30% CR, started at age 8–14 yrs) to mitigate the loss of muscle mass, it was concluded that CR did not alter the frequency of fibers (type I or II) showing age-associated loss of mitochondrial function (McKiernan et al.; McKiernan et al.). In humans, CR increased mtDNA in muscle homogenates but was without effect on Vmax of several mitochondrial enzymes (Civitarese et al., 2007). In rhesus monkeys, there was in fact a decrease in expression of oxidative phosphorylation genes in *vastus lateralis* with long term CR; however, this decrease was similar to that occurring with aging alone (Kayo et al., 2001). In that study, no beneficial effects of CR were observed in gene expression in *vastus lateralis*, leading the authors to conclude that species differences or an effect of age of onset of CR may impact the skeletal muscle response. We too have noted species differences in the effect of CR on skeletal muscle mitochondrial H^+ leak and ROS production in Wt mice and rats (Bevilacqua et al., 2005; Bevilacqua et al., 2010). Our study within the same species suggests that CR effects in muscle depend on the initial physiological state, which could explain some apparent species differences.

The findings in muscle are largely in contrast to the increase in mitochondrial mass with CR that has been reported for brain, liver, brown adipose tissue and the heart (Nisoli et al., 2005). While CR can induce some functional changes in skeletal muscle mitochondria (present study; (Asami et al., 2008; Barazzoni et al., 2005; Bevilacqua et al., 2004, 2005; Civitarese et al., 2007)), our results in murine skeletal muscle (short duration CR), together with the abovementioned observations from skeletal muscle of rats, monkeys and humans (longer duration CR), are inconsistent with the concept that a feature of CR is an extensive remodelling of the mitochondrial mass in all tissues. The latter conclusion was also very recently reached from an analysis of different tissues in 3 mo CR rats (Hancock et al., 2011). Our observations from muscle-specific UCP3Tg mice suggest, however, that mitochondrial function influences the response to CR. Another point is that while frequency of abnormal mitochondrial enzyme activity in *Vastus lateralis* increased with age in control monkeys, it was not correlated with age in CR monkeys (McKiernan et al.). In rats, accumulation with age of defective mitochondrial enzyme activity was delayed by CR (40% CR, started at 14

wks of age) (Bua et al., 2004). Also in rats, while activity of various mitochondrial enzymes as lower with CR, there was no age-dependent decline in activity in CR rats (Baker et al., 2006). These time course studies suggest that an important effect of CR on skeletal muscle mitochondria may be to mitigate the age-dependent decline in mitochondrial function.

The present study, like many of the cited studies in rodents (Faulks et al., 2006; Hancock et al., 2011; Lee et al., 1999; Sreekumar et al., 2002), starts the CR regime at an age when the animals are still growing. It is possible that CR initiated in 12 wk old mice induced starvation, because mice at this age are still growing. To determine whether this was a factor, we measured naso-anal and femur length at the time of sacrifice. There were no significant differences with 2 wks or 1 mo CR in either genotype (Supplemental Table 3). Thus skeletal growth was not compromised by CR. We also note that white adipose tissue depots had not been exhausted by 1 mo CR and that the RER data indicate that, even at the end of 1 mo CR, the mice could switch to fat oxidation. Although these observations suggest that CR mice were not in a chronic state of starvation, the possibility that mitochondrial content is differently affected by CR in young and old mice should be addressed in a dedicated study.

4.3. Impact of UCP3/uncoupling on muscle adaptation

In AL-fed mice, the phenotype associated with muscle-specific overexpression of UCP3Tg was increased basal H^+ leak and decreased ROS emission in isolated skeletal muscle mitochondria, and, at the whole-body level, decreased BW. This phenotype, which overlaps with that produced by exogenous administration of uncouplers (Caldeira da Silva et al., 2008), was associated with a slightly different pattern of response to 2 wk CR in UCP3Tg mice. Strikingly, these differences countered aspects of the AL phenotype in these mice: ROS emission increased and basal H^+ leak was lowered by 2 wk CR. The mechanisms responsible for these changes are not clear. The lower ANT protein and decreased leak could each be linked with high ROS emission. Yet it seems unlikely that the lower leak would explain the decreased ROS in the presence of antimycin since, under that condition, the membrane potential is depolarized, whereas leak would be expected to impact ROS at hyperpolarized potentials. Since ANT can regulate basal H^+ leak (Brand et al., 2005), the slight decrease in ANT protein may be partially responsible for the lowered leak. Interestingly, H^+ leak in muscle mitochondria increased in UCP3 knockout mice after 2 wk CR (Bevilacqua et al., 2010). Thus, while UCP3 protein abundance may not be responsible for lowered H^+ leak, UCP3 function may modulate leak. In this regard, we have recently demonstrated that glutathionylation of UCP3 can regulate leak (Mailloux et al.). The partial recovery of the CR response by 1 month in UCP3Tg mice cannot be explained by the present study. Though highly speculative, one possibility is a role for ROS-dependent signalling in the CR response. Because ROS emission and leak (which would regulate ROS) differ in UCP3Tg mice, processes dependent on ROS signalling may also differ in these mice.

Generally, these findings indicate that UCP3/uncoupling can influence the adaptive response of muscle. Indeed, UCP3 overexpression mitigates some of the deleterious effects of high fat feeding (Choi et al., 2007; Costford et al., 2008; Costford et al., 2006; Tiraby et al., 2007),

and UCP3 knockout is associated with increased ROS production in permeabilized muscle from exercise-challenged mice (Anderson et al., 2007), and in mitochondria from fasted mice (Seifert et al., 2008). Our present results, together with the ones just mentioned, raise the general question of whether administration of a chemical uncoupler or an agent to activate uncoupling proteins, as CR mimetics, will impact the adaptive capacity of skeletal muscle.

In conclusion, UCP3 overexpression and/or its associated phenotypes appear to delay some aspects of the CR response. This finding of delayed adaptation in UCP3Tg mice raises the general question of how pharmacologic uncoupling would impact other adaptive responses. While uncoupling may be beneficial in some cases such as with the ability of muscle to adapt to a high fat diet, the present study suggests that the impact could be to delay adaptive changes to some challenges. In addition to the primary goal of our study, we also present strong evidence that short term CR, as with longer term CR, is not associated with an extensive remodelling of the mitochondria nor an increase in mitochondrial content in mouse skeletal muscle; thus, the remodelling reported to occur in other tissues does not reflect a fundamental response to CR in mice.

Highlights

1. We test if similar mechanisms drive adaptation to mitochondrial uncoupling and CR.
2. We use a mouse model of skeletal muscle-targeted UCP3 overexpression (UCP3Tg).
3. UCP3Tg CR mice adapted differently to CR following both 2 weeks and 1 month CR.
4. Strikingly, muscle mitochondria of control mice changed minimally with CR.
5. We conclude that uncoupling and CR depend on distinct mechanisms.

Supplementary Material

Refer to Web version on PubMed Central for supplementary material.

Acknowledgments

We wish to thank Linda Jui, Jian Xuan and Amanda Daniels for expert technical assistance, and Dr. Véronic Bezaire for careful reading of the manuscript and helpful discussions. We also thank Dr. Luke Szweda (Oklahoma Medical Research Foundation) for the gift of the aconitase and 4-HNE antibodies. This study was supported in part by NIH R01AG030226, and by the National Science and Engineering Council (NSERC) of Canada. ELS was supported by a fellowship from the Canadian Diabetes Association.

References

Smith DL Jr, Nagy TR, Allison DB. Calorie restriction: what recent results suggest for the future of ageing research. Eur J Clin Invest. 2010; 40:440–450. [PubMed: 20534066]

Heilbronn LK, de Jonge L, Frisard MI, DeLany JP, Larson-Meyer DE, Rood J, Nguyen T, Martin CK, Volaufova J, Most MM, Greenway FL, Smith SR, Deutsch WA, Williamson DA, Ravussin E.

Effect of 6-month calorie restriction on biomarkers of longevity, metabolic adaptation, and oxidative stress in overweight individuals: a randomized controlled trial. JAMA. 2006; 295:1539–1548. [PubMed: 16595757]

Chen D, Guarente L. SIR2: a potential target for calorie restriction mimetics. Trends Mol Med. 2007; 13:64–71. [PubMed: 17207661]

Ingram DK, Zhu M, Mamczarz J, Zou S, Lane MA, Roth GS, deCabo R. Calorie restriction mimetics: an emerging research field. Aging Cell. 2006; 5:97–108. [PubMed: 16626389]

Caldeira da Silva CC, Cerqueira FM, Barbosa LF, Medeiros MH, Kowaltowski AJ. Mild mitochondrial uncoupling in mice affects energy metabolism, redox balance and longevity. Aging Cell. 2008; 7:552–560. [PubMed: 18505478]

Mookerjee SA, Divakaruni AS, Jastroch M, Brand MD. Mitochondrial uncoupling and lifespan. Mech Ageing Dev. 2010; 131:463–472. [PubMed: 20363244]

Barazzoni R, Zanetti M, Bosutti A, Biolo G, Vitali-Serdoz L, Stebel M, Guarnieri G. Moderate caloric restriction, but not physiological hyperleptinemia per se, enhances mitochondrial oxidative capacity in rat liver and skeletal muscle--tissue-specific impact on tissue triglyceride content and AKT activation. Endocrinology. 2005; 146:2098–2106. [PubMed: 15618355]

Bevilacqua L, Ramsey JJ, Hagopian K, Weindruch R, Harper ME. Effects of short- and medium-term calorie restriction on muscle mitochondrial proton leak and reactive oxygen species production. Am J Physiol Endocrinol Metab. 2004; 286:E852–E861. [PubMed: 14736705]

Bevilacqua L, Ramsey JJ, Hagopian K, Weindruch R, Harper ME. Long-term caloric restriction increases UCP3 content but decreases proton leak and reactive oxygen species production in rat skeletal muscle mitochondria. Am J Physiol Endocrinol Metab. 2005; 289:E429–E438. [PubMed: 15886224]

Civitarese AE, Carling S, Heilbronn LK, Hulver MH, Ukropcova B, Deutsch WA, Smith SR, Ravussin E. Calorie restriction increases muscle mitochondrial biogenesis in healthy humans. PLoS Med. 2007; 4:e76. [PubMed: 17341128]

Marzetti E, Lawler JM, Hiona A, Manini T, Seo AY, Leeuwenburgh C. Modulation of age-induced apoptotic signaling and cellular remodeling by exercise and calorie restriction in skeletal muscle. Free Radic Biol Med. 2008; 44:160–168. [PubMed: 18191752]

Nisoli E, Tonello C, Cardile A, Cozzi V, Bracale R, Tedesco L, Falcone S, Valerio A, Cantoni O, Clementi E, Moncada S, Carruba MO. Calorie restriction promotes mitochondrial biogenesis by inducing the expression of eNOS. Science. 2005; 310:314–317. [PubMed: 16224023]

Asami DK, McDonald RB, Hagopian K, Horwitz BA, Warman D, Hsiao A, Warden C, Ramsey JJ. Effect of aging, caloric restriction, and uncoupling protein 3 (UCP3) on mitochondrial proton leak in mice. Exp Gerontol. 2008; 43:1069–1076. [PubMed: 18852040]

Guarente L. Mitochondria--a nexus for aging, calorie restriction, and sirtuins? Cell. 2008; 132:171–176. [PubMed: 18243090]

Hancock CR, Han DH, Higashida K, Kim SH, Holloszy JO. Does calorie restriction induce mitochondrial biogenesis? A reevaluation. FASEB J. 2011; 25:785–791. [PubMed: 21048043]

Lass A, Sohal BH, Weindruch R, Forster MJ, Sohal RS. Caloric restriction prevents age-associated accrual of oxidative damage to mouse skeletal muscle mitochondria. Free Radic Biol Med. 1998; 25:1089–1097. [PubMed: 9870563]

Korshunov SS, Skulachev VP, Starkov AA. High protonic potential actuates a mechanism of production of reactive oxygen species in mitochondria. FEBS Lett. 1997; 416:15–18. [PubMed: 9369223]

Seifert EL, Estey C, Xuan JY, Harper ME. Electron transport chain-dependent and -independent mechanisms of mitochondrial H2O2 emission during long-chain fatty acid oxidation. J Biol Chem. 2010; 285:5748–5758. [PubMed: 20032466]

Gates AC, Bernal-Mizrachi C, Chinault SL, Feng C, Schneider JG, Coleman T, Malone JP, Townsend RR, Chakravarthy MV, Semenkovich CF. Respiratory uncoupling in skeletal muscle delays death and diminishes age-related disease. Cell Metab. 2007; 6:497–505. [PubMed: 18054318]

Katterle Y, Keipert S, Hof J, Klaus S. Dissociation of obesity and insulin resistance in transgenic mice with skeletal muscle expression of uncoupling protein 1. Physiol Genomics. 2008; 32:352–359. [PubMed: 18042832]

Li B, Nolte LA, Ju JS, Han DH, Coleman T, Holloszy JO, Semenkovich CF. Skeletal muscle respiratory uncoupling prevents diet-induced obesity and insulin resistance in mice. Nat Med. 2000; 6:1115–1120. [PubMed: 11017142]

Neschen S, Katterle Y, Richter J, Augustin R, Scherneck S, Mirhashemi F, Schurmann A, Joost HG, Klaus S. Uncoupling protein 1 expression in murine skeletal muscle increases AMPK activation, glucose turnover, and insulin sensitivity in vivo. Physiol Genomics. 2008; 33:333–340. [PubMed: 18349383]

Padalko VI. Uncoupler of oxidative phosphorylation prolongs the lifespan of Drosophila. Biochemistry (Mosc). 2005; 70:986–989. [PubMed: 16266268]

Fridell YW, Sanchez-Blanco A, Silvia BA, Helfand SL. Targeted expression of the human uncoupling protein 2 (hUCP2) to adult neurons extends life span in the fly. Cell Metab. 2005; 1:145–152. [PubMed: 16054055]

Speakman JR, Talbot DA, Selman C, Snart S, McLaren JS, Redman P, Krol E, Jackson DM, Johnson MS, Brand MD. Uncoupled and surviving: individual mice with high metabolism have greater mitochondrial uncoupling and live longer. Aging Cell. 2004; 3:87–95. [PubMed: 15153176]

Clapham JC, Arch JR, Chapman H, Haynes A, Lister C, Moore GB, Piercy V, Carter SA, Lehner I, Smith SA, Beeley LJ, Godden RJ, Herrity N, Skehel M, Changani KK, Hockings PD, Reid DG, Squires SM, Hatcher J, Trail B, Latcham J, Rastan S, Harper AJ, Cadenas S, Buckingham JA, Brand MD, Abuin A. Mice overexpressing human uncoupling protein-3 in skeletal muscle are hyperphagic and lean. Nature. 2000; 406:415–418. [PubMed: 10935638]

Chappell JB, Perry SV. Biochemical and osmotic properties of skeletal muscle mitochondria. Nature. 1954; 173:1094–1095. [PubMed: 13165721]

Dubowitz, V.; Sewry, CA. Muscle Biopsy: A practical Approach. Third ed.. Elsevier Limited; 2007.

Tsai L, Szweda PA, Vinogradova O, Szweda LI. Structural characterization and immunochemical detection of a fluorophore derived from 4-hydroxy-2-nonenal and lysine. Proc Natl Acad Sci U S A. 1998; 95:7975–7980. [PubMed: 9653125]

Bezaire V, Spriet LL, Campbell S, Sabet N, Gerrits M, Bonen A, Harper ME. Constitutive UCP3 overexpression at physiological levels increases mouse skeletal muscle capacity for fatty acid transport and oxidation. FASEB J. 2005; 19:977–979. [PubMed: 15814607]

Costford SR, Chaudhry SN, Crawford SA, Salkhordeh M, Harper ME. Long-term high-fat feeding induces greater fat storage in mice lacking UCP3. Am J Physiol Endocrinol Metab. 2008; 295:E1018–E1024. [PubMed: 18713955]

Costford SR, Chaudhry SN, Salkhordeh M, Harper ME. Effects of the presence, absence, and overexpression of uncoupling protein-3 on adiposity and fuel metabolism in congenic mice. Am J Physiol Endocrinol Metab. 2006; 290:E1304–E1312. [PubMed: 16434555]

Bevilacqua L, Seifert EL, Estey C, Gerrits MF, Harper ME. Absence of uncoupling protein-3 leads to greater activation of an adenine nucleotide translocase-mediated proton conductance in skeletal muscle mitochondria from calorie restricted mice. Biochim Biophys Acta. 2010; 1797:1389–1397. [PubMed: 20206124]

Brand MD, Pakay JL, Ocloo A, Kokoszka J, Wallace DC, Brookes PS, Cornwall EJ. The basal proton conductance of mitochondria depends on adenine nucleotide translocase content. Biochem J. 2005; 392:353–362. [PubMed: 16076285]

Choi CS, Fillmore JJ, Kim JK, Liu ZX, Kim S, Collier EF, Kulkarni A, Distefano A, Hwang YJ, Kahn M, Chen Y, Yu C, Moore IK, Reznick RM, Higashimori T, Shulman GI. Overexpression of uncoupling protein 3 in skeletal muscle protects against fat-induced insulin resistance. J Clin Invest. 2007; 117:1995–2003. [PubMed: 17571165]

Tiraby C, Tavernier G, Capel F, Mairal A, Crampes F, Rami J, Pujol C, Boutin JA, Langin D. Resistance to high-fat-diet-induced obesity and sexual dimorphism in the metabolic responses of transgenic mice with moderate uncoupling protein 3 overexpression in glycolytic skeletal muscles. Diabetologia. 2007; 50:2190–2199. [PubMed: 17676309]

Baker DJ, Betik AC, Krause DJ, Hepple RT. No decline in skeletal muscle oxidative capacity with aging in long-term calorically restricted rats: effects are independent of mitochondrial DNA integrity. J Gerontol A Biol Sci Med Sci. 2006; 61:675–684. [PubMed: 16870628]

Lambert AJ, Wang B, Yardley J, Edwards J, Merry BJ. The effect of aging and caloric restriction on mitochondrial protein density and oxygen consumption. Exp Gerontol. 2004; 39:289–295. [PubMed: 15036388]

Sreekumar R, Unnikrishnan J, Fu A, Nygren J, Short KR, Schimke J, Barazzoni R, Nair KS. Effects of caloric restriction on mitochondrial function and gene transcripts in rat muscle. Am J Physiol Endocrinol Metab. 2002; 283:E38–E43. [PubMed: 12067840]

Lee CK, Klopp RG, Weindruch R, Prolla TA. Gene expression profile of aging and its retardation by caloric restriction. Science. 1999; 285:1390–1393. [PubMed: 10464095]

Colman RJ, Anderson RM, Johnson SC, Kastman EK, Kosmatka KJ, Beasley TM, Allison DB, Cruzen C, Simmons HA, Kemnitz JW, Weindruch R. Caloric restriction delays disease onset and mortality in rhesus monkeys. Science. 2009; 325:201–204. [PubMed: 19590001]

Faulks SC, Turner N, Else PL, Hulbert AJ. Calorie restriction in mice: effects on body composition, daily activity, metabolic rate, mitochondrial reactive oxygen species production, and membrane fatty acid composition. J Gerontol A Biol Sci Med Sci. 2006; 61:781–794. [PubMed: 16912094]

McKiernan SH, Colman RJ, Aiken E, Evans TD, Beasley TM, Aiken JM, Weindruch R, Anderson RM. Cellular adaptation contributes to calorie restriction-induced preservation of skeletal muscle in aged rhesus monkeys. Exp Gerontol.

McKiernan SH, Colman RJ, Lopez M, Beasley TM, Aiken JM, Anderson RM, Weindruch R. Caloric restriction delays aging-induced cellular phenotypes in rhesus monkey skeletal muscle. Exp Gerontol. 46:23–29. [PubMed: 20883771]

Evans WJ. What is sarcopenia? J Gerontol A Biol Sci Med Sci. 1995; 50(Spec No, 5–8)

Kayo T, Allison DB, Weindruch R, Prolla TA. Influences of aging and caloric restriction on the transcriptional profile of skeletal muscle from rhesus monkeys. Proc Natl Acad Sci U S A. 2001; 98:5093–5098. [PubMed: 11309484]

Bua E, McKiernan SH, Aiken JM. Calorie restriction limits the generation but not the progression of mitochondrial abnormalities in aging skeletal muscle. FASEB J. 2004; 18:582–584. [PubMed: 14734641]

Mailloux RJ, Seifert EL, Bouillaud F, Aguer C, Collins S, Harper ME. Glutathionylation acts as a control switch for uncoupling proteins UCP2 and UCP3. J Biol Chem. 286:21865–21875. [PubMed: 21515686]

Anderson EJ, Yamazaki H, Neufer PD. Induction of endogenous uncoupling protein 3 suppresses mitochondrial oxidant emission during fatty acid-supported respiration. J Biol Chem. 2007; 282:31257–31266. [PubMed: 17761668]

Seifert EL, Bezaire V, Estey C, Harper ME. Essential role for uncoupling protein-3 in mitochondrial adaptation to fasting but not in fatty acid oxidation or fatty acid anion export. J Biol Chem. 2008; 283:25124–25131. [PubMed: 18628202]

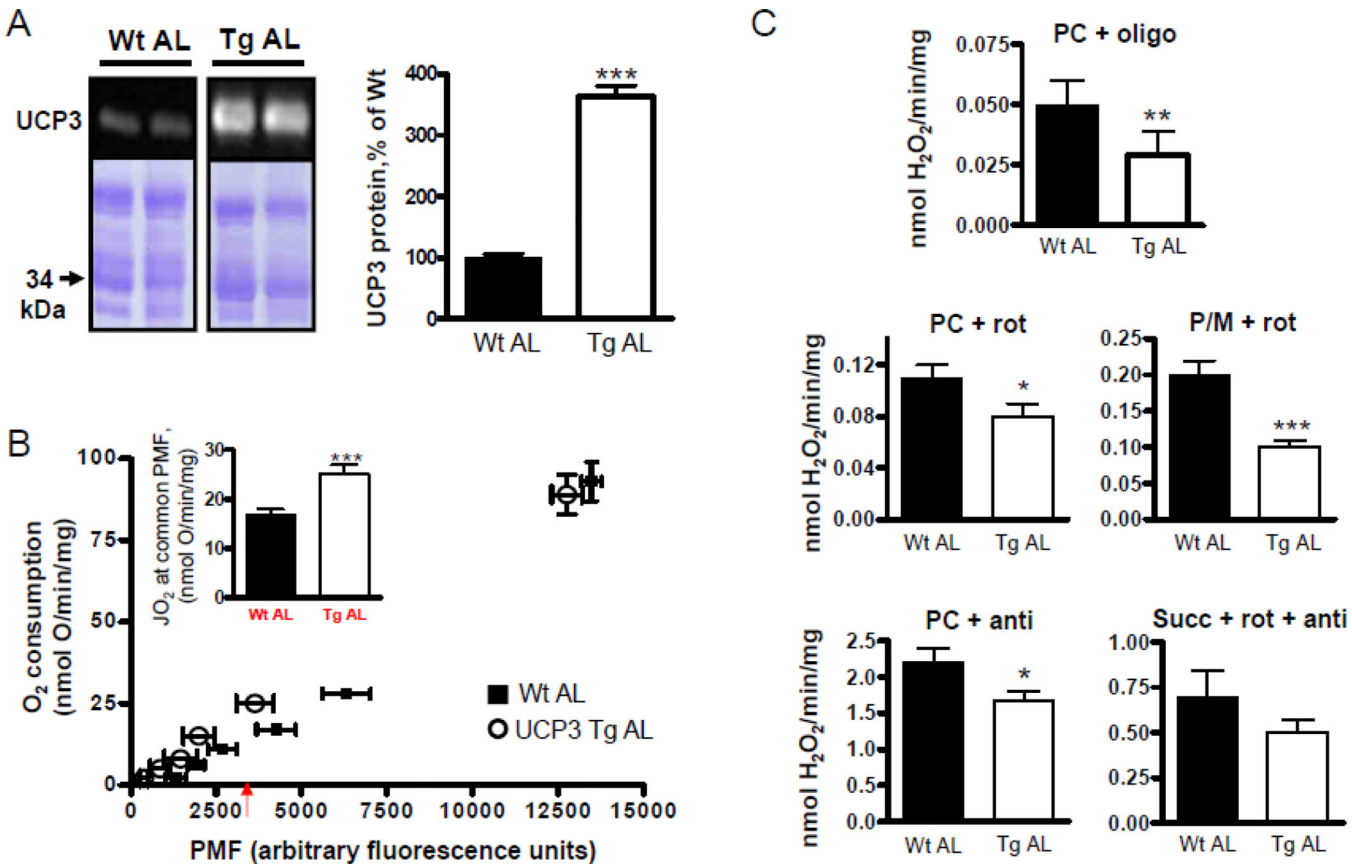

Figure 1. Characteristics of UCP3Tg skeletal muscle mitochondria from AL-fed mice

(A) Expression of UCP3 protein in mitochondria from AL-fed (AL) Wt and UCP3Tg mice. Lower bands are from Coomassie (G-250)-stained gel. Right panel shows quantification, expressed as % of Wt. For each sample, the UCP3 band was normalized to bands of similar MW on the Coomassie-stained gel. *** $P < 0.001$, unpaired t-test, n=8/genotype. (B) Proton leak kinetics in mitochondria (0.3mg/ml) from AL-fed Wt (closed squares) and UCP3Tg (open circles) mice, determined by parallel measurements of O_2 consumption (JO_2; Clark electrode) and protonmotive force (PMF; fluorimetrically using 5μM safranin). Succinate (10mM) was used as the substrate; then ETC activity was titrated by 1mM malonate additions. Rotenone (5μM) and nigericin (0.4μg/ml) were also present. The rightmost point represents state 4. Inset: JO_2 at common PMF (indicated by arrow beneath x-axis) shows increased basal H^+ leak in UCP3Tg mitochondria. *** $P < 0.001$, unpaired t-test, n=3–4/genotype. (C) H_2O_2 emission in mitochondria (0.3mg/mL) from AL-fed Wt and UCP3Tg mice, as measured by the PHPA/HRP method, using different substrate and inhibitor combinations. PC: palmitoyl-L-carnitine (18μM); P/M: pyruvate/malate (5mM/2.5mM); succ: succinate (10mM); oligo: oligomycin (8μg/mg mitochondria); rot: rotenone (5μM); anti: antimycin (5μM); SOD: superoxide dismutase (20U/ml). *: $P < 0.05$, **: $P < 0.01$; ***: $P < 0.001$, unpaired t-test, n=4–6/group. All values: mean±SEM.

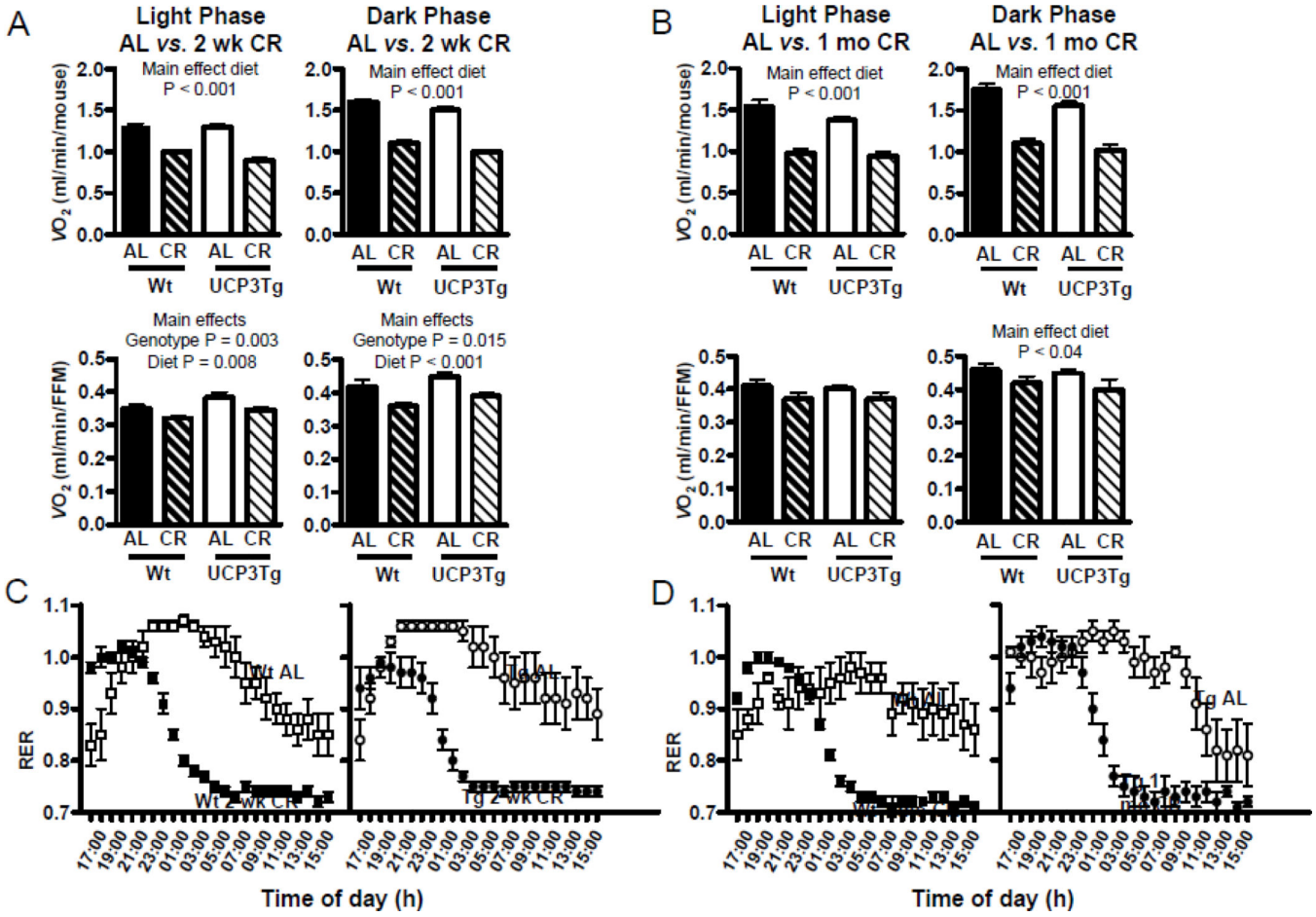

Figure 2. CR effects on whole-body oxygen consumption and fuel selection in Wt and UCP3Tg mice

Effect of 2 wk (A) and 1 mo (B) CR on whole-body oxygen consumption (VO_2), expressed per mouse (top panels) or per fat free mass (FFM; lower panels). FFM was determined by the sum of skeletal muscle, liver, kidneys, and heart. Analysis: two-way ANOVA, P values for main effects; 2-wk CR: n=8–10/group; 1-mo CR: n=5/group. (C) and (D) Respiratory exchange ratios; chow was provided at 16:00. No significant differences between genotypes; two-way ANOVA; 2 wk CR: n=8–10/group; 1 mo CR: n=5/group. All values: mean ± SEM.

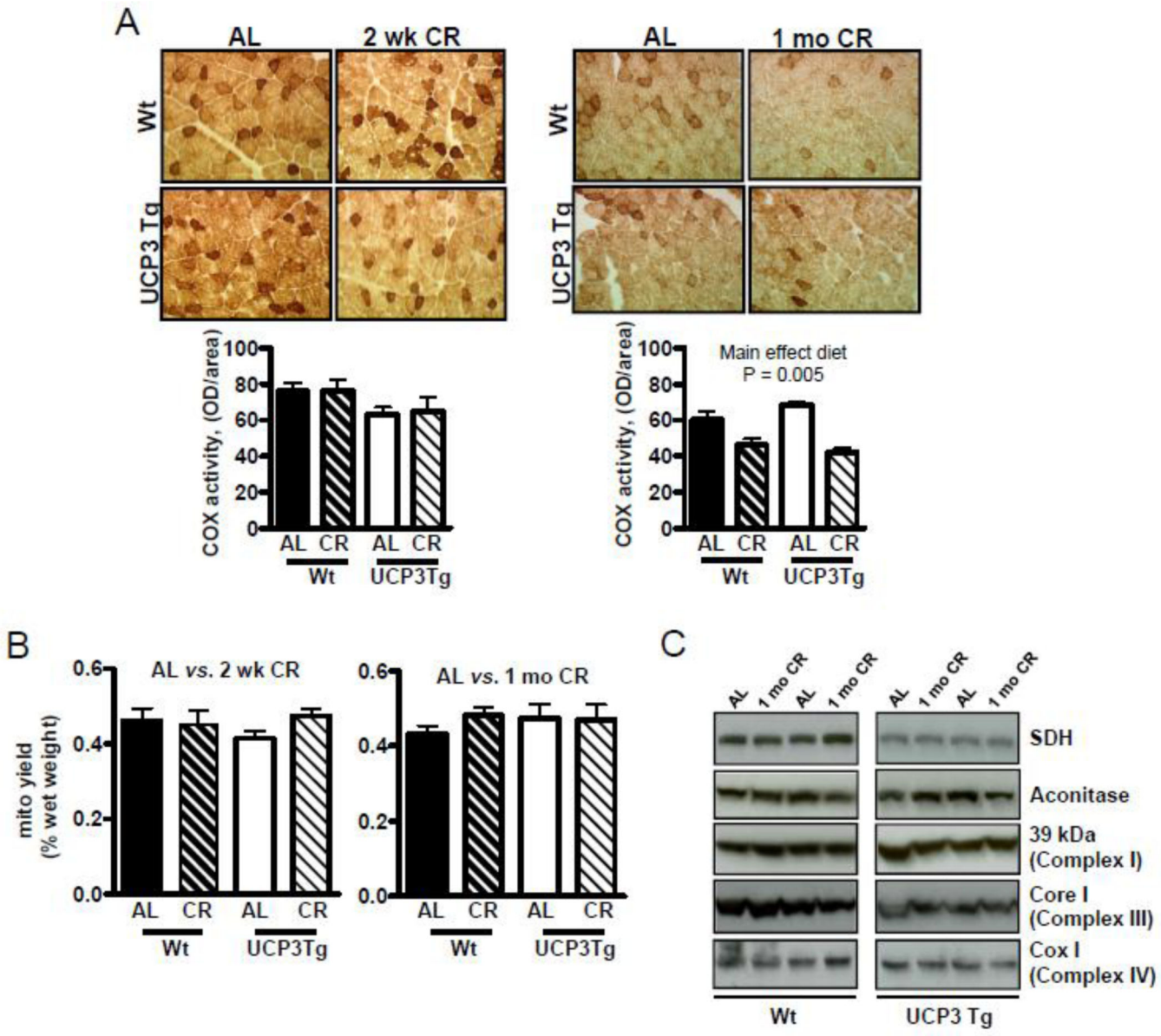

Figure 3. Similar mitochondrial content in skeletal muscle from Wt and UCP3Tg mice challenged with 2 wk or 1 mo CR

(A) Histochemical activity staining of cytochrome c oxidase in quadriceps muscle. Staining was quantified by determining the optical density (OD) per total area of muscle analyzed. Analysis: two-way ANOVA, P values are for main effects; n=5/group. (B) Mitochondrial yield, expressed per muscle wet weight; 2 wk CR: n=10/group; 1 mo CR: n=7/group. (C) Levels of tricarboxylic acid cycle and electron transport chain proteins from homogenates of quadriceps muscle, by Western blotting. In (B) and (C), significant differences were not found; two-way ANOVA (quantification of Western blots not shown; n=6/group). All values: mean ± SEM.

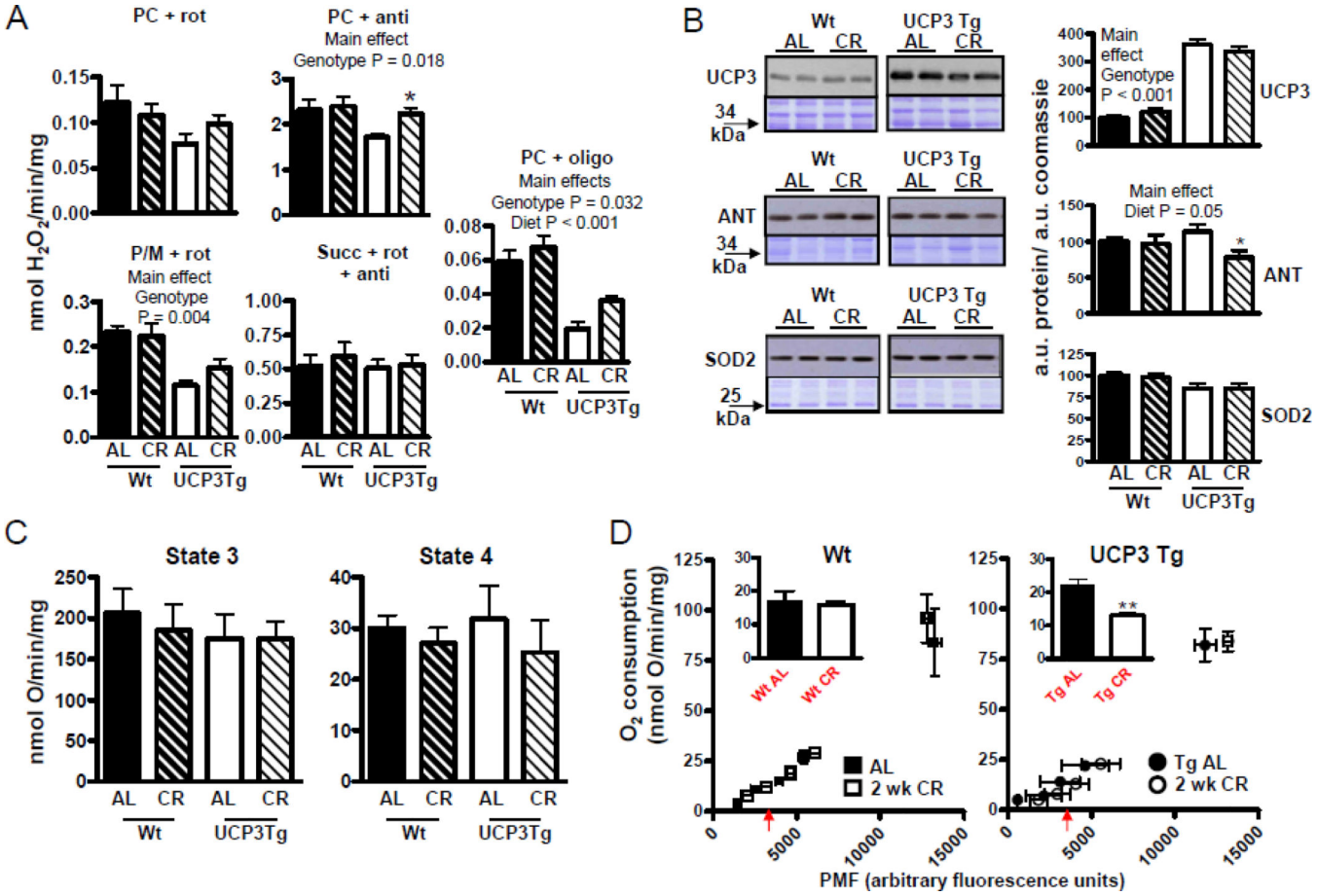

Figure 4. Differential impact of 2 wk CR on intrinsic function of skeletal muscle mitochondria from Wt and UCP3Tg mice

(A) H_2O_2 emission, determined as described in Fig. 1; see Fig. 1 for abbreviations. Analyses by two-way ANOVA; P values for main effects; *: difference between Wt and UCP3Tg CR response at the 99% confidence level; n=4–7/group. (B) Levels of anti-oxidant proteins, by Western blotting. Left panels: Upper panels show immunoblot; lower panels show Coomassie-stained gel at similar MW as protein band. Right panels show quantification: all values were divided through by the amount of protein loaded (as determined by the Coomassie stained gel). Analyses by two-way ANOVA, P values for main effects. UCP3: n=7–8/group; ANT: n=5–7/group; MnSOD: n=5–7/group. CR caused a decrease in ANT protein in UCP3 Tg mice: *: difference between Wt and UCP3Tg CR response at the 99% confidence level. (C) Bioenergetic characteristics of mitochondria (0.25 mg/mL), using pyruvate (5mM) and malate (2.5mM) used as the substrate. Left panel: maximal phosphorylating respiration (state 3), induced using saturating ADP (200μM) (n=7–10/group). Right panel: non–phosphorylating respiration (state 4), induced by oligomycin (8μg/mg mitochondria) (n=6–10/group). No detectable CR effects on state 3 or 4 oxygen consumption in either genotype. (D) Proton leak kinetics, as described in Fig. 1 (also see Methods). Inset: oxygen consumption at a common PMF (~3500 a.u., as indicated by the arrow beneath the x-axis). 2 wk CR resulted in decreased in leak in UCP3Tg but not Wt mitochondria; **:P=0.02, unpaired t-test; n=3–4/group. All values: mean±SEM.

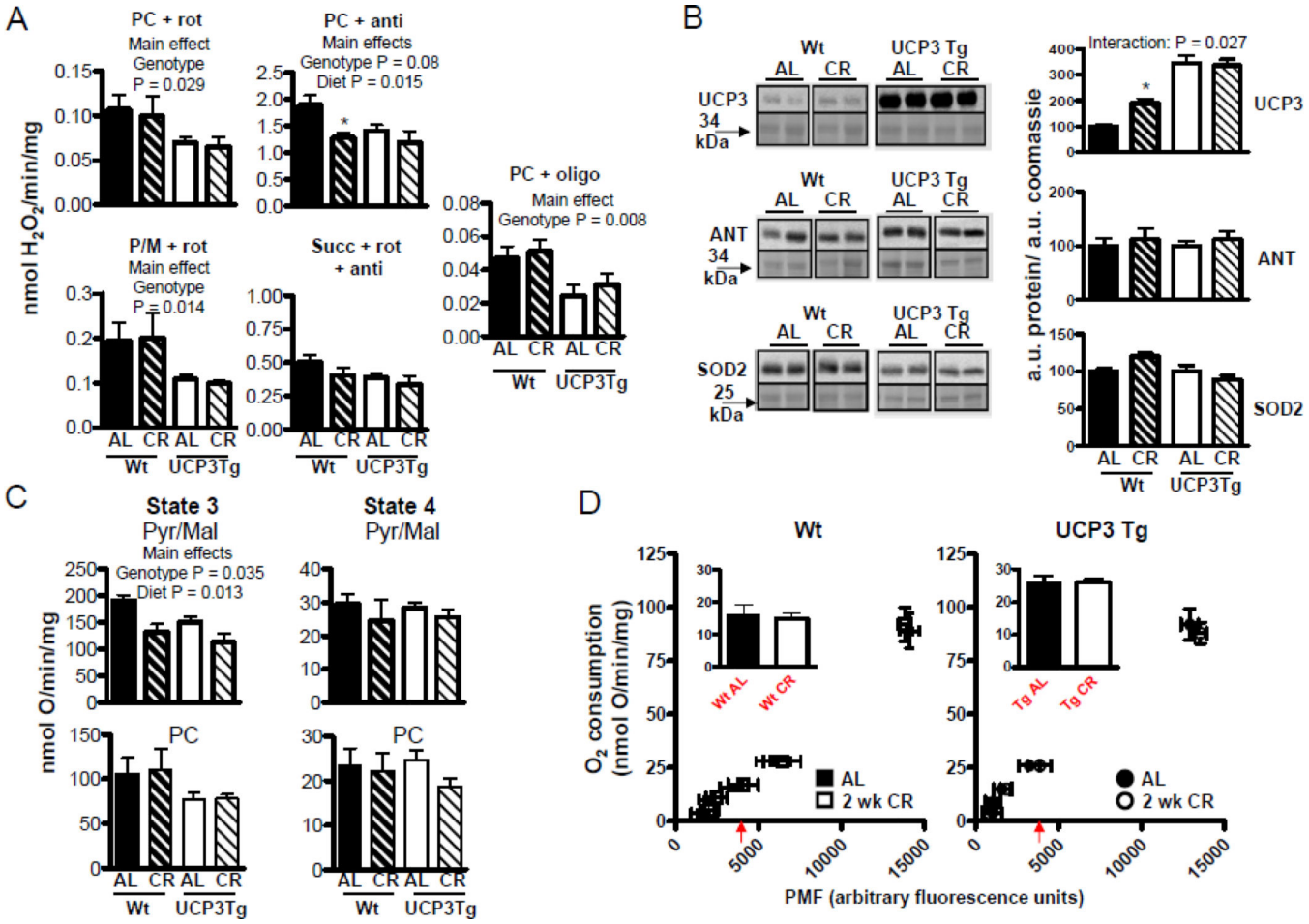

Figure 5. Impact of 1 mo CR on intrinsic function of skeletal muscle mitochondria from Wt and UCP3Tg mice

(A) H_2O_2 emission, as described in Fig. 1; see Fig. 1 for abbreviations. CR induced a decrease in ROS production in Wt mice with PC (+antimycin) as substrate; Analyses by two–way ANOVA, P values are for main effects; *: difference between Wt and UCP3Tg CR response at the 97.5% confidence level n=6/group. (B) Levels of anti-oxidant proteins, by Western blotting. Left panels: in all cases, AL and CR samples from a given genotype were from the same blot. Upper panels show immunoblot; lower panels show Coomassie-stained gel at similar MW as protein band. Right panels show quantification: all values were divided through by the amount of protein loaded (as determined by the Coomassie stained gel). Analyses by two-way ANOVA: significant genotype X diet interaction for UCP3. UCP3; n=4–8/group; ANT: n=5–7/group; MnSOD (Mn-superoxide dismutase); n=5–7/group. (C) Bioenergetic characteristics of mitochondria (0.25mg/mL), using pyruvate/malate (pyr/mal; 5mM/2.5mM) (top panels) or palmitoyl-L-carnitine (PC;18μM). Left panels: maximal phosphorylating respiration (state 3), induced using saturating ADP (200μM) (n=7–10/group). Right panel: non–phosphorylating respiration (state 4), induced by oligomycin (8μg/mg mitochondria) (n=6–10/group). Analyses by two-way ANOVA, P values for main effects. (D) Proton leak kinetics, as described in Fig. 1 (also see Methods). Inset: oxygen

consumption at a common PMF (~3500 a.u., as indicated by the arrow beneath the x-axis). All values: mean±SEM.

Table 1

Body and organ weights in *ad libitum*-fed (AL) and in 2 week 40% calorie restricted (CR) Wt and UCP3Tg mice. Values: means±sem. Analysis by 2-way ANOVA; P values are for main effects of genotype, diet and genotype X diet. *Ad libitum* food intake prior to CR is also shown (last row). Upper table: absolute values. Lower table: organ weights as a fraction of body weight.

2 week CR	**Wt AL**	**Wt CR**	**UCP3Tg AL**	**UCP3Tg CR**	**P value: main effect of genotype**	**P value: main effect of diet**	**P value: genotype X diet**
Liver, g	1.32 ± 0.03	0.82 ± 0.02	1.21 ± 0.08	0.79 ± 0.03	0.16	<0.0001	0.44
Kidney, g	0.31 ± 0.01	0.25 ± 0.01	0.31 ± 0.02	0.24 ± 0.00	0.49	<0.0001	0.41
Heart, g	0.13 ± 0.00	0.12 ± 0.00	0.13 ± 0.00	0.11 ± 0.00	0.44	0.0003	0.49
gWAT, g	0.71 ± 0.08	0.31 ± 0.04	0.65 ± 0.09	0.16 ± 0.02	0.11	<0.0001	0.55
iBAT, g	0.18 ± 0.01	0.11 ± 0.00	0.17 ± 0.01	0.09 ± 0.01	0.14	<0.0001	0.33
Muscle, g	2.07 ± 0.11	1.83 ± 0.04	1.71 ± 0.04	1.43 ± 0.02	<0.0001	0.0004	0.73
Body weight, g	28.5 ± 0.6	21.3 ± 0.6	25.0 ± 0.6	18.5 ± 0.2	<0.0001	<0.0001	0.46
Food intake (g/day)	2.72 ± 0.04 (g/day)		2.77 ± 0.05 (g/day)				
Food intake (g/day/BW)	0.112 ± 0.001 (g/day/BW)		0.118 ± 0.001*** (g/day/BW)				
2 week CR	Wt AL	Wt CR	UCP3Tg AL	UCP3Tg CR	P value: main effect of genotype	P value: main effect of diet	P value: genotype X diet
Liver, g	4.8 ± 0.13	3.9 ± 0.05	4.8 ± 0.29	3.3 ± 0.23	0.13	<0.0001	0.18
Kidney, g	1.1 ± 0.03	1.2 ± 0.02	1.2 ± 0.05	1.0 ± 0.05	0.22	0.035	0.0014
Heart, g	0.5 ± 0.03	0.6 ± 0.01	0.5 ± 0.02	0.5 ± 0.03	0.26	0.55	0.01
gWAT, g	2.6 ± 0.21	1.5 ± 0.16	2.5 ± 0.24	0.7 ± 0.12	0.04	0.0001	0.073
iBAT, g	0.6 ± 0.03	0.5 ± 0.02	0.7 ± 0.04	0.4 ± 0.03***	0.028	<0.0001	0.002
Muscle, g	7.5 ± 0.30	8.8 ± 0.15	6.9 ± 0.30	6.0 ± 0.25***	<0.0001	0.43	0.0003

*** P = 0.001, unpaired t-test.

Table 2

Body and organ weights in *ad libitum*-fed (AL) and in 1 month 40% calorie restricted (CR) Wt and UCP3Tg mice. Values: means±sem. Analysis by 2-way ANOVA. P values are for main effects of genotype, diet and genotype X diet. *Ad libitum* food intake prior to CR is also shown. Upper table: absolute values. Lower table: organ weights as a fraction of body weight.

1 month CR	**Wt AL**	**Wt CR**	**UCP3Tg AL**	**UCP3Tg CR**	**P value: main effect of genotype**	**P value: main effect of diet**	**P value: genotype X diet**
Liver, g	1.21 ± 0.09	0.75 ± 0.04	1.15 ± 0.11	0.74 ± 0.06	0.67	<0.0001	0.72
Kidney, g	0.34 ± 0.01	0.24 ± 0.01	0.33 ± 0.02	0.25 ± 0.02	0.86	<0.0001	0.38
Heart, g	0.12 ± 0.00	0.10 ± 0.00	0.12 ± 0.01	0.10 ± 0.00	0.64	0.006	0.70
gWAT, g	1.25 ± 0.19	0.15 ± 0.03	0.86 ± 0.05	0.21 ± 0.05	0.17	<0.0001	0.068
iBAT, g	0.17 ± 0.03	0.08 ± 0.01	0.18 ± 0.02	0.07 ± 0.01	0.9	<0.0001	0.78
Muscle, g	2.13 ± 0.05	1.56 ± 0.05	1.84 ± 0.05	1.46 ± 0.07	0.0024	<0.0001	0.10
Body weight, g	31.4 ± 1.05	19.5 ± 0.58	27.3 ± 0.93	18.1 ± 0.34	0.0015	<0.0001	0.10
Food intake (g/day)	2.98 ± 0.05		2.92 ± 0.05				
Food intake (g/day)	0.118 ± 0.002 (g/day/BW)		0.127 ± 0.002*** (g/day/BW)				
1 month CR	Wt AL	Wt CR	UCP3Tg AL	UCP3Tg CR	P value: main effect of genotype	P value: main effect of diet	P value: genotype X diet
Liver, g	3.8 ± 0.10	3.8 ± 0.19	4.2 ± 0.42	4.0 ± 0.29	0.27	0.79	0.77
Kidney, g	1.1 ± 0.05	1.3 ± 0.04	1.2 ± 0.03	1.4 ± 0.09	0.11	0.01	0.77
Heart, g	0.4 ± 0.02	0.5 ± 0.01	0.4 ± 0.02	0.5 ± 0.02	0.042	<0.0001	0.40
gWAT, g	3.9 ± 0.63	0.8 ± 0.17	3.1 ± 0.35	1.1 ± 0.24	0.52	<0.001	0.14
iBAT, g	0.5 ± 0.05	0.4 ± 0.03	0.6 ± 0.05	0.4 ± 0.07	0.11	0.004	0.32
Muscle, g	6.9 ± 0.27	8.1 ± 0.21	6.7 ± 0.30	8.0 ± 0.25	0.55	0.002	0.95

*** P = 0.001, unpaired t-test.